High resolution double-sided diffractive optics for hard X-ray microscopy

Istvan Mohacsi,[1,2,*] **Ismo Vartiainen,**[1] **Manuel Guizar-Sicairos,**[1] **Petri Karvinen,**[1,3] **Vitaliy A. Guzenko,**[1] **Elisabeth Müller,**[1] **Elina Färm,**[4] **Mikko Ritala,**[4] **Cameron M. Kewish,**[2] **Andrea Somogyi**[2] **and Christian David**[1]

[1]*Paul Scherrer Institut, 5232 Villigen PSI, Switzerland*
[2]*Synchrotron SOLEIL, L'Orme des Merisiers, 91190 Saint-Aubin, France*
[3]*University of Eastern Finland, Institute of Photonics, PL 111 FI-80101 Joensuu, Finland*
[4]*University of Helsinki, A.I.Virtasen aukio 1, FI-00014 Helsinki, Finland*
[*]*istvan.mohacsi@psi.ch*

Abstract: The fabrication of high aspect ratio metallic nanostructures is crucial for the production of efficient diffractive X-ray optics in the hard X-ray range. We present a novel method to increase their structure height via the double-sided patterning of the support membrane. In transmission, the two Fresnel zone plates on the two sides of the substrate will act as a single zone plate with added structure height. The presented double-sided zone plates with 30 nm smallest zone width offer up to 9.9% focusing efficiency at 9 keV, that results in a factor of two improvement over their previously demonstrated single-sided counterparts. The increase in efficiency paves the way to speed up X-ray microscopy measurements and allows the more efficient utilization of the flux in full-field X-ray microscopy.

OCIS codes: (050.1965) Diffractive lenses; (050.1970) Diffractive optics; (340.7460) X-ray microscopy; (220.4241) Nanostructure fabrication

References and links

1. G. Porod, "Die Rontgenkleinwinkelstreuung von dichtgepackten kolloiden Systemen I. Teil (X-ray low angle scattering of dense colloid systems. Part I.)," Kolloid-Zeitschrift **124**, 83–114 (1951).
2. H. D. Bale and P. W. Schmidt, "Small-Angle X-Ray-Scattering Investigation of Submicroscopic Porosity with Fractal Properties," Physical Review Letters, **53**, 596 (1984).
3. M. R. Howells, T. Beetz, H. N. Chapman, C. Cui, J. M. Holton, C. J. Jacobsen, J. Kirz, E. Lima, S. Marchesini, H. Miao, D. Sayre, D. A. Shapiro, J. C. H. Spence and D. Starodub, "An assessment of the resolution limitation due to radiation-damage in X-ray diffraction microscopy," Journal of Electron Spectroscopy and Related Phenomena **170**, 4–12 (2009).
4. P. Kirkpatrick and A. V. Baez, "Formation of Optical Images by X-Rays," J. Opt. Soc. Am. **38**(9), 766–774 (1948).
5. A. Snigirev, V. Kohn, I. Snigireva and B. Lengeler, "A compound refractive lens for focusing high-energy X-rays," Nature **384**, 49–51 (1996).
6. J. Maser, G. B. Stephenson, S. Vogt, W. Yun, A. Macrander, H. C. Kang, C. Liu, R. Conley, "Multilayer Laue lenses as high-resolution x-ray optics," Proc. SPIE **5539**, 185–194 (2004).
7. J. L. Soret, "Ueber die von Kreisgittern erzeugten Diffraktionsphaenomene", Ann. Phys. Chem, **156**, 99 (1875).
8. J. Kirz, "Phase zone plates for x rays and the extreme UV," J. Opt. Soc. Am. **20**(3), 301–309 (1974).
9. S.-R. Wu and Y. Hwu and G. Margaritondo, "Hard-X-ray Zone Plates: Recent Progress," Materials, **5**, 1752–1773 (2012).
10. B. L. Henke, E. M. Gullikson and J. C. Davis, "X-ray interactions: photoabsorption, scattering, transmission, and reflection at E=50-30000 eV, Z=1-92," Atomic Data and Nuclear Data Tables **54**(2), 181–342 (1993).

#224406 - $15.00 USD Received 6 Oct 2014; revised 28 Nov 2014; accepted 1 Dec 2014; published 13 Jan 2015

11. S. Gorelick, V. A. Guzenko, J. Vila-Comamala and C. David, "Direct e-beam writing of dense and high aspect ratio nanostructures in thick layers of PMMA for electroplating," Nanotechnology **21**, 295303 (2010).
12. W. Chao, B. D. Harteneck, J. Alexander Liddle, Erik H. Anderson and David T. Attwood, "Soft X-ray microscopy at a spatial resolution better than 15nm," Nature **435**, 1210–1213 (2005).
13. F. Uhlen, D. Nilsson, J. Rahomaki, L. Belova, C. G. Schroer, F. Seiboth, A. Holmberg, H. M. Hertz and U. Vogt, "Nanofabrication of tungsten zone plates with integrated platinum central stop for hard X-ray applications", Microelectronic Engineering **116**, 40–43 (2014).
14. Y. Feng, M. Feser, A. Lyon, S. Rishton, X. Zeng, S. Chen, S. Sassolini and W. Yun, "Nanofabrication of high aspect ratio 24 nm x-ray zone plates for x-ray imaging applications," Journal of Vacuum Science and Technology B **25**, 2004 (2007).
15. C. David, B. Nöhammer and E. Ziegler, "Wavelength tunable diffractive transmission lens for hard x rays," Applied Physics Letters **79**, 1088–1090 (2001).
16. C. Chang and A. Sakdinawat, "Ultra-high aspect ratio high-resolution nanofabrication for hard X-ray diffractive optics," Nature Communications **5**, 4243 (2014).
17. S. Werner, S. Rehbein, P. Guttmann and G. Schneider, "Three-dimensional structured on-chip stacked zone plates for nanoscale X-ray imaging with high efficiency," Nano Research **7**(4), 1–8 (2014).
18. F. Döring, A. L. Robisch, C. Eberl, M. Osterhoff, A. Ruhlandt, T. Liese, F. Schlenkrich, S. Hoffmann, M. Bartels, T. Salditt and H.U. Krebs, "Sub-5 nm hard x-ray point focusing by a combined Kirkpatrick-Baez mirror and multilayer zone plate," Opt. Express **21**(16), 19311–19323 (2013).
19. J. Maser, B. Lai, W. Yun, S. D. Shastri, Z. Cai, W. Rodrigues, S. Xua and E. Trackhtenberg, "Near-field stacking of zone plates in the x-ray range," Proc. SPIE, **4783**, 74 (1999).
20. I. Snigireva, A. Snigirev, V. Kohn, V. Yunkin, M. Grigoriev, S. Kuznetsov, G. Vaughan and M. Di Michiel, "Focusing high energy X-rays with stacked Fresnel zone plates," physica status solidi (a) **204**(8), 2817–2823 (2007).
21. A. G. Michette, *Optical Systems for Soft X Rays* (Plenum Press, 1986).
22. K. Jefimovs, J. Vila-Comamala, T. Pilvi, J. Raabe, M. Ritala and C. David, "Zone-Doubling Technique to Produce Ultrahigh-Resolution X-Ray Optics," Physical Review Letters **99**, 264801 (2007).
23. J. Vila-Comamala, S. Gorelick, E. Färm, C. M. Kewish, A. Diaz, R. Barrett, V. A. Guzenko, M. Ritala and C. David, "Ultra-high resolution zone-doubled diffractive X-ray optics for the multi-keV regime," Opt. Express **19**(1) 175–184 (2011).
24. J. Vila-Comamala, S. Gorelick, V. A. Guzenko, E. Färm, M. Ritala and C. David, "Dense high aspect ratio hydrogen silsesquioxane nanostructures by 100 keV electron beam lithography," Nanotechnology **21**, 285305 (2010).
25. V. A. Guzenko, J. Romijn, J. Vila-Comamala, S. Gorelick and C. David, "Efficient E-Beam Lithography Exposure Strategies for Diffractive X-ray Optics," AIP Conf. Proc. **1365**, 92 (2012).
26. T. Aaltonen, M. Ritala, V. Sammelselg and M. Leskela, "Atomic Layer Deposition of Iridium Thin Films," Journal of The Electrochemical Society **151**(8), 489–492 (2004).
27. J. M. Rodenburg, A. C. Hurst, A. G. Cullis, B. R. Dobson, F. Pfeiffer, O. Bunk, C. David, K. Jefimovs and I. Johnson, "Hard-x-ray lensless imaging of extended objects," Physical Review Letters **98**, 34801 (2007).
28. B. Henrich, A. Bergamaschi, C. Broennimann, R. Dinapoli, E.F. Eikenberry, I. Johnson, M. Kobas, P. Kraft, A. Mozzanica and B. Schmitt, "PILATUS: A single photon counting pixel detector for X-ray applications," Nuclear Instruments and Methods in Physics Research Section A **607**(1), 247–249 (2009).
29. M. Guizar-Sicairos and J. R. Fienup, "Phase retrieval with transverse translation diversity: a nonlinear optimization approach," Opt. Express **16**(10), 7264–7278 (2008).
30. P. Thibault, M. Dierolf, A. Menzel, O. Bunk, C. David and F. Pfeiffer, "High-Resolution Scanning X-ray Diffraction Microscopy," Science **321**, 379–382 (2008).
31. P. Thibault, M. Dierolf, O. Bunk, A. Menzel and F. Pfeiffer, "Probe retrieval in ptychographic coherent diffractive imaging," Ultramicroscopy **109**(4), 338–343 (2009).
32. J. Vila-Comamala, A. Diaz, M. Guizar-Sicairos, A. Mantion, C. M. Kewish, A. Menzel, O. Bunk and C. David, "Characterization of high-resolution diffractive X-ray optics by ptychographic coherent diffractive imaging," Opt. Express **19**(22), 21333–21344 (2011).
33. C. M. Kewish, M. Guizar-Sicairos, C. Liu, J. Qian, B. Shi, C. Benson, A. M. Khounsary, J. Vila-Comamala, O. Bunk, J. R. Fienup, A. T. Macrander and L. Assoufid "Reconstruction of an astigmatic hard X-ray beam and alignment of K-B mirrors from ptychographic coherent diffraction data," Opt. Express **18**(22), 23420–23427 (2010).
34. E. Wolf and M. Born, *Principles of Optics (1st edition)* (Pergamon Press Ltd. 1959), p. 415.
35. K. Strehl, "Aplanatische und fehlerhafte Abbildung im Fernrohr," Zeitschrift fur Instrumentenkunde **15**, 362–370 (1895).
36. James C. Wyant and Katherine Creath, "Basic Wavefront Aberration Theory for Optical Metrology," Applied Optics and Optical Engineering **11** (1992).
37. M. J. Simpson and A. G. Michette, "Imaging Properties of Modified Fresnel Zone Plates," Optica Acta **31**(4), 403–413 (1984).

#224406 - $15.00 USD Received 6 Oct 2014; revised 28 Nov 2014; accepted 1 Dec 2014; published 13 Jan 2015

38. M. Guizar-Sicairos, M. Holler, A. Diaz, J. Vila-Comamala, O. Bunk and A. Menzel, "Role of the illumination spatial-frequency spectrum for ptychography," Phys. Rev. B **86**, 100103 (2012).

1. Introduction

Hard X-ray microscopy comprises several analytical techniques, providing the possibility of imaging highly heterogeneous, organic or inorganic samples using high energy photons. It takes advantage of the high penetration depth, high resolution and chemical sensitivity of X-rays and allows studying extended samples without extensive sample preparation. Experimental methods include scanning probe microscopy, full field microscopy and coherent diffractive imaging, often combined with tomography or time resolved measurements. The resolution of X-ray microscopes typically falls between the resolution of electron and optical microscopy, yet its resolution is limited in radiation sensitive, e.g. biological, specimens. On one hand, according to the Debye-Porod law, the required dose to distinguish smaller features is inversely proportional to the fourth power of the feature size [1, 2]. On the other hand, radiation damage limits the total dose that can be applied to the samples before they are degraded by radiation damage, leading to the loss of fine details in recorded images [3].

Hard X-rays can be focused via KB mirrors [4], compound refractive lenses [5] or multilayer Laue lenses [6] as well as with Fresnel zone plates (FZP) [7]. The latter group consists of stigmatic, compact and easy to handle optical elements which are commonly used from the extreme UV [8] to the hard X-ray range [9]. Their compact dimensions allows great flexibility in their use, as they can fill their role as a focusing lens for micro- and nanoprobe experiments as well as to serve as an objective lens for full field X-ray microscopes. However, their focusing efficiency, defined as the fraction of the incoming flux that can be used for imaging, is limited. It is related to the fabrication properties and the structure height of the zone plate through the optical constants of the zone plate material [8, 10].

The focusing efficiency of Fresnel zone plates increases quadratically with the structure height for optically shallow structures and in case of no absorption it reaches its maximum at the height corresponding to π phase shift as shown on Fig. 1. The optimal structure height of heavy metals typically falls in the range of microns in the multi-keV range. Higher photon energies require even taller structures to obtain a reasonable focusing efficiency. Additionally, the resolution of zone plate optics is on the order of their smallest zone width when using their most efficient 1^{st} diffraction order. Therefore, the fabrication of high efficiency and high resolution Fresnel zone plate lenses requires the production of heavy metal nanostructures with high aspect ratios. Due to the fabrication limitations, high resolution zone plates have only a few percent efficiency in the hard X-ray range [9]. Their low photon efficiency becomes particularly problematic in full field microscopy. The objective zone plate uses only a small fraction of the illuminating flux for imaging while the total incoming intensity contributes to the radiation damage. This makes the fabrication of efficient high resolution Fresnel zone plates a key element towards improving photon efficiency, and considering radiation damage, also the achievable resolution [3] in hard X-ray microscopy.

Various processes have been described in the literature to yield dense and high aspect ratio metallic nanostructures as required for zone plate fabrication. For the production of zone plates electroplating [11, 12], dry etching [13, 14] and wet etching [15, 16] have been all proven as successful techniques. However, if high resolution is needed, the previous methods have serious issues with producing nanostructures with sufficient structure height. The use of multiple patterning steps can increase structure height, however the demonstrated methods [17] require many fabrication steps to reach high aspect ratios, making them vulnerable to fabrication issues. Other emerging methods, like multilayer deposition on a wire substrate, have been shown to produce virtually unlimited aspect ratios, but thus far their aperture size is insufficient for

#224406 - $15.00 USD Received 6 Oct 2014; revised 28 Nov 2014; accepted 1 Dec 2014; published 13 Jan 2015

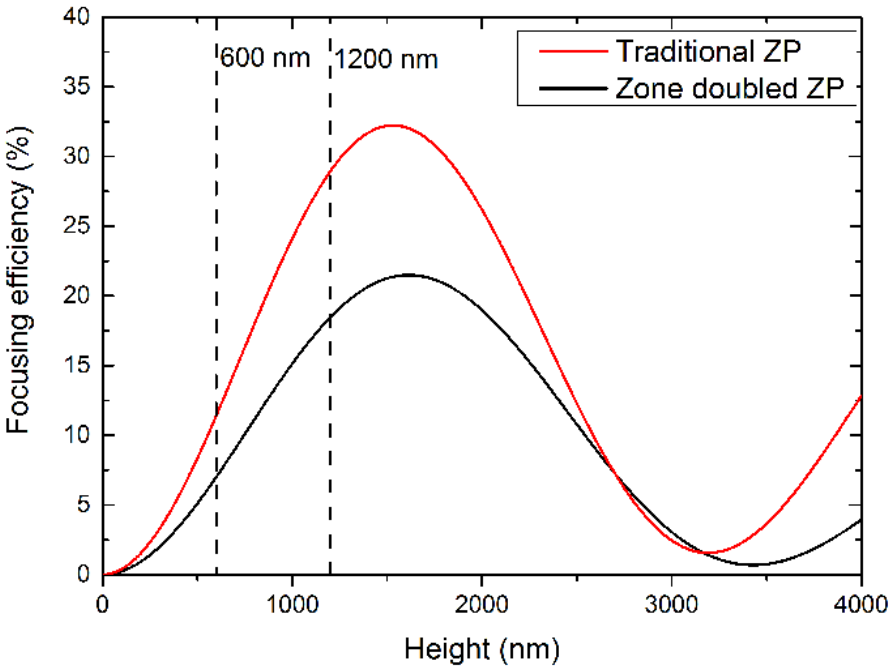

Fig. 1. The calculated theoretical focusing efficiency of a traditional and a line-doubled iridium zone plate versus the structure height at 9 keV photon energy. The focusing efficiency increases steeply with increasing structure height. Doubling the height of 600 nm tall structures results in a factor of 2.5 increase in efficiency. The gain would be even larger at higher photon energies. The overall efficiency of line doubled zone plates is lower, as the deposition thickness provides optimal fill factor only in the outer zones (see Fig. 2). This makes the contribution of the central zones negligible when summing up the efficiency.

most practical applications [18].

The effective structure height of a single zone plate can be improved by mechanically stacking two zone plates. By placing two identical zone plates in each other's optical near field, they act as a single zone plate with added zone height [19]. This prompted several scientists [14, 20] to permanently glue together a stack of two zone plates using epoxy resin to create a monolithic, single-chip device. As the required alignment accuracy for stacking is $1/3$ of the smallest zone width [21], these zone plate stacks must be aligned and glued within the X-ray beam. Any stress in the glue can cause a drift during or after the curing, degrading optical performance [20].

In this paper we demonstrate a new concept to improve the efficiency of high resolution zone plate optics by the independent but aligned double-sided patterning of silicon nitride membranes using electron beam lithography. Patterning both sides of the support membrane with the identical zone plates leads to doubled effective structure height similar to zone plate stacking. This allows effective aspect ratios that would have been impossible to produce in a single step. Furthermore, these lenses are inherently produced as monolithic, single chip optical elements and without the need for alignment in the X-ray beam and the risk of subsequent drift.

The fabrication process for each of the two zone plates is based on direct patterning of a sparse, high aspect ratio hydrogen-silsesquioxane (HSQ) resist template and conformally coating it with heavy metals using atomic layer deposition [22, 23]. The heavy metal coating on both template walls doubles the effective line density and hence resolution. The deposited thickness

#224406 - $15.00 USD Received 6 Oct 2014; revised 28 Nov 2014; accepted 1 Dec 2014; published 13 Jan 2015

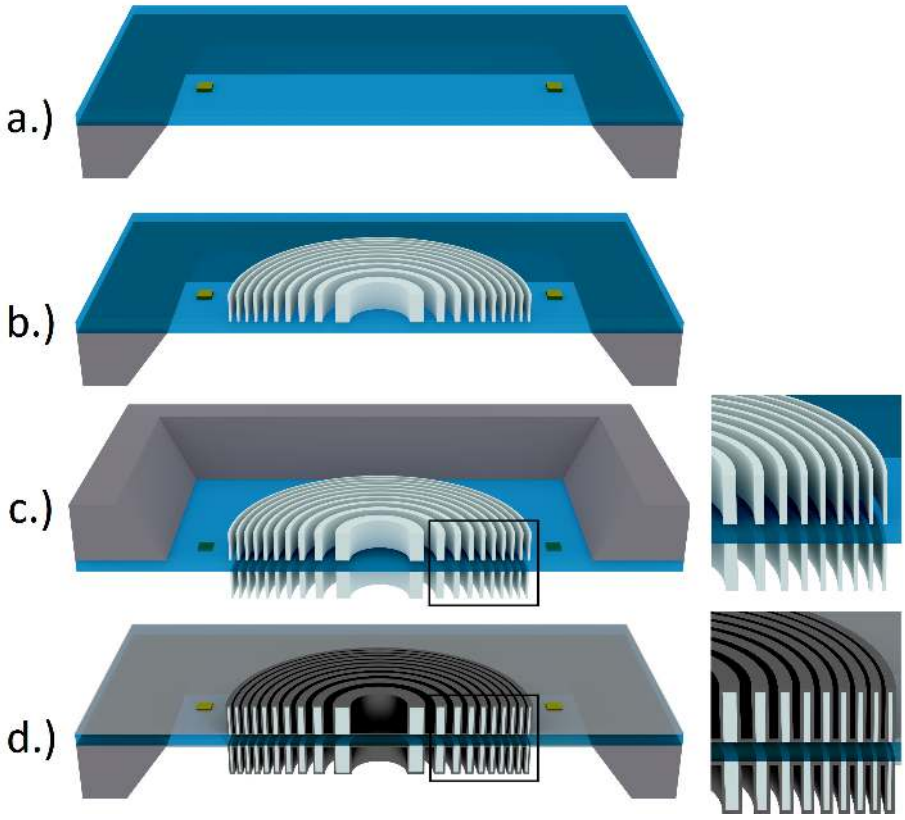

Fig. 2. Schematic fabrication process of the presented double-sided line-doubled Fresnel zone plates. (a) The membranes are patterned with gold alignment markers. (b) The patterning of the resist template on the front side is aligned on the markers. (c) Since the markers can be located through the membrane, the resist template on the back side is also patterned using the same alignment markers as for the front side. (d) The double-sided resist template is then conformally coated by iridium using atomic layer deposition.

should be set to provide optimal fill factor for the smaller zones of the zone plate, thus sacrificing efficiency in the large inner zones, this effect is apparent in Fig. 1. By patterning two of these line-doubled zone plates on the same substrate, as illustrated on Fig. 2., we can surpass previously demonstrated aspect ratios. This allows us to significantly improve focusing efficiencies in the hard X-ray range, while preserving the high image quality, associated with e-beam patterned zone plates.

Our substrates were 250 nm thick and 2 mm x 2 mm sized rectangular silicon nitride membranes, coated with 20 nm gold and 5 nm chromium layer on both sides. Prior to the exposures of the actual zone plates, we patterned sets of gold alignment markers on our membranes [11]. We patterned our zone plates by 100 keV electron beam lithography using a Vistec EBPG 5000+ ES tool using direct writing [25, 24].

For the patterning of the zone plates, we coated our chips with $\sim$ 600 nm of HSQ resist (FOX 16, Dow Corning) on the processed side. The spin-coating of the back side was done by mounting the chip on a chuck having a central recess in order to prevent the membrane area from touching the chuck surface. Droplets of resist were applied on the membranes; excessive resist was quickly removed by using high acceleration settings. We observed that the

#224406 - $15.00 USD Received 6 Oct 2014; revised 28 Nov 2014; accepted 1 Dec 2014; published 13 Jan 2015

obtained thicknesses on the back sides of the membranes were about 20% thicker than on the front side. As the electron beam writer could clearly locate our markers through the membrane, we aligned both the front and back side exposures on the very same set of markers using the e-beam writer's built-in alignment procedure. Each membrane was patterned with several zone plates of 100 micron diameter and 30 nm smallest zone width using different exposure dose and line width. After the exposure, the samples were developed in a buffered NaOH developer (Microposit A351 : H_2O, 1:3) for 20 minutes, followed by rinsing in water and isopropanol. The samples were dried by supercritical drying to avoid collapse of the high aspect ratio nanostructures [24]. The same process was repeated independently for the front and the back sides. The prepared resist template was finally conformally coated with $\sim$ 35 nm iridium using atomic layer deposition [26].

In order to test the thickness and conformity of the deposited iridium layer and obtain information about the structure quality, selected zone plates were cut with focused ion beam (FIB) to inspect the zone profile. As shown in Fig. 3., the cross section of the zone plate shows large contrast between the empty trenches (dark), the resist template (dark) and the iridium coated sidewalls (bright). The iridium is conformal, covering the resist template in uniform thickness on both the front and the back side. The heights of the two sides add up in transmission, resulting in a total of $\sim$ 1200 nm effective structure height for the 30 nm zones, corresponding to aspect ratios close to 40. The zones are vertical to the membrane and appear to be in excellent alignment on the opposite sides.

2. Results and discussion

The efficiency of the produced double-sided line-doubled Fresnel zone plates was measured at the cSAXS beamline of the Swiss Light Source and the Nanoscopium beamline of the synchrotron SOLEIL. Additional STXM and ptychography measurements shown here were performed at the cSAXS beamline. The zone plates were tested at 9 keV X-ray photon energy. The performance of the best zone plates was further evaluated in X-ray applications, including scanning transmission X-ray microscopy and ptychographic coherent diffractive imaging [27].

We measured the diffraction efficiency of our zone plates by selecting the primary diffraction order using a 10 micron pinhole. This allowed us to measure the focused flux on a Pilatus 2M [28] single photon counting pixel detector placed far downstream of the focus. The focused flux was normalized into efficiency by calibrating the Pilatus with photodiode based efficiency measurements. The 0th order radiation was masked out and subtracted, from the measurements, but no central stop was used to block the inefficient central part of the zone plates. The average diffraction efficiency of 95 measured double-sided zone plates was 7.6% at 9 keV with the best zone plate having 9.9% diffraction efficiency (as seen in Fig. 4). In comparison, the highest focusing efficiency previously reported for single-sided iridium zone plates with similar zone width was 5.1% [23]. The factor of two gain in focusing efficiency shows the clear advantage of increased structure height at higher photon energies, in agreement with Fig. 1.The measured spread in focusing efficiency also showed strong correlation with the exposure dose. Too wide resist lines due to overdose or beam forward scattering lead to a misplacement of the Iridium zones deposited on the sidewalls of the resist structures. This misplacement enhances other diffraction orders at the expense of the first diffraction order. This is the main reason why only $\sim$ 50% of the theoretical efficiency is obtained in the primary focus on both the single- and double- sided zone plates.

The recorded light cone on the pixel detector also represents a spatial map of diffraction efficiency, allowing us to evaluate the radial dependence of focusing efficiency as seen on Fig. 4. We see gradual decrease in efficiency towards the zone plate center that is expected for line-doubled zone plates, as the deposited iridium layer only provides optimal fill factor at

#224406 - $15.00 USD Received 6 Oct 2014; revised 28 Nov 2014; accepted 1 Dec 2014; published 13 Jan 2015

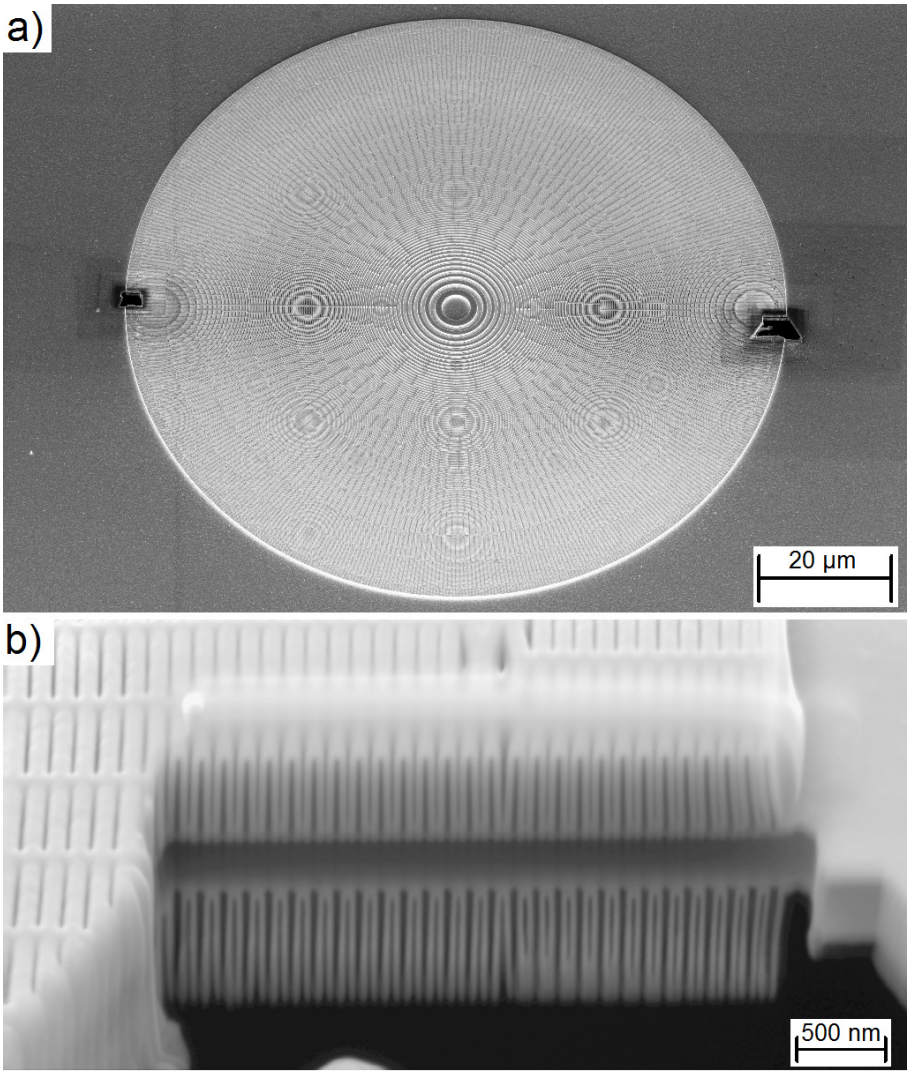

Fig. 3. Scanning electron microscope images from the FIB sliced double-sided line-doubled zone plates. (a) Overview of a double-sided line-doubled Fresnel zone plate, showing the large central structures and cuts, made by focused ion beam (FIB) on the zone plate edge. (b) FIB cross section of a double-sided zone doubled Fresnel zone plate. The highly scattering Ir coating (bright) conformally covers the template on both sides of the membrane with a uniform thickness on both sides. The two zone plates are in an excellent alignment to each other, no misalignment can be measured from the cross section. By combining the two zone plates on the opposite sides of the membrane, the total height of the iridium sidewalls is $\sim$ 1200 nm, resulting in an effective aspect ratio of $\sim$ 40 for 30 nm smallest zone width.

#224406 - $15.00 USD Received 6 Oct 2014; revised 28 Nov 2014; accepted 1 Dec 2014; published 13 Jan 2015

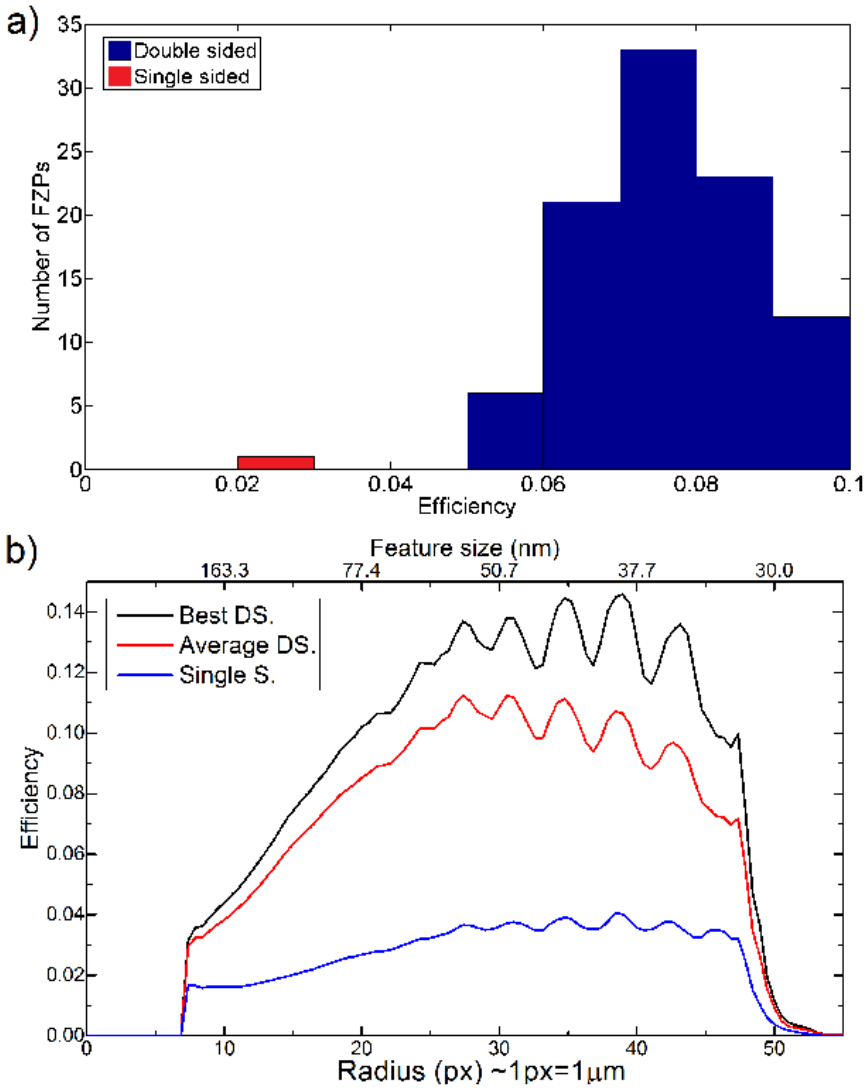

Fig. 4. (a) Efficiency histogram of the measured zone plates at 9 keV. The average focusing efficiency of the 95 double-sided zone plates (blue) was 7.6% . The single-sided reference zone plate had 2.8% (red), while the best double-sided zone plate had 9.9% focusing efficiency. The majority of the double-sided zone plates performed in the $7-8\%$ range. (b) The radial efficiency distribution of the tested zone plates. The efficiency decreases towards the large central zones but even the smallest outer zones exhibit high diffraction efficiency, providing high contrast for imaging high spatial frequencies. The error induced by the radial support structures [32] is also clearly visible as quasi-periodic oscillations in efficiency.

#224406 - $15.00 USD Received 6 Oct 2014; revised 28 Nov 2014; accepted 1 Dec 2014; published 13 Jan 2015

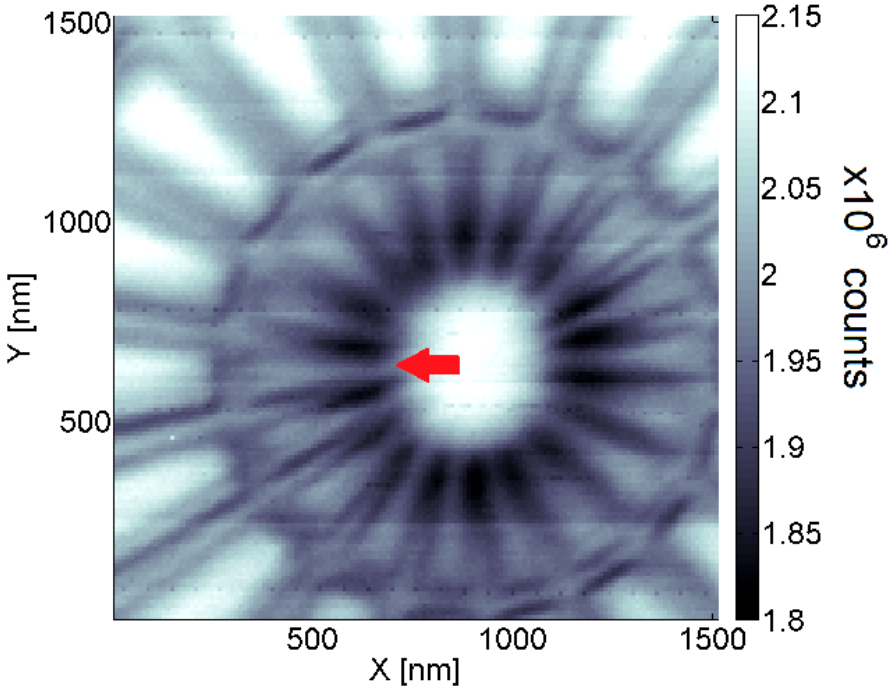

Fig. 5. Scanning transmission X-ray microscope image of a line-doubled Siemens star using the best performing zone plate. With a step size of 10 nm, the smallest spokes of 30 nm lines and spaces were resolved (marked by the arrow), demonstrating that our zone plates indeed match their expected resolution.

the outermost zones. Nevertheless, the efficiency remains high towards the zone plate edge, which is essential to provide strong contrast at high spatial frequencies. The light cones are also rotationally symmetric, no Moire-patterns [19] are visible. This implies that the alignment accuracy of our zone plates was well below than the required 10 nm [21].

We tested the performance of our zone plates by scanning transmission X-ray microscopy. Therefore we blocked the 0th diffraction order using a 40 micron diameter central stop and scanned a high resolution Siemens star as a test object. Fig. 5. shows that by using a scan with 150x150 points and 10 nm step size, the 30 nm spokes of the Siemens star are resolved. This proves that our lenses indeed match their predicted resolution.

As the focal spot shape is a key performance indicator of high resolution Fresnel zone plate optics, we performed additional characterization to identify possible errors in the lens wavefield. X-ray ptychography is a phase sensitive coherent diffractive imaging method [27], that can simultaneously recover both the measured object and the illuminating wavefield [29, 30, 31]. The reconstructed illumination can be then propagated back to the focal plane to characterize the illuminating optics [31, 32, 33]. We moved the test object 400 microns downstream of the focus and performed ptychographic scans on 2x2 μm^2 areas consisting of 284 diffraction patterns for all measured zone plates. The retrieved illumination was propagated back to the focal plane, as shown for example in Fig. 6(a). The measured focal spot of the best zone plate, shown on Fig. 6(b) and (c), closely matches the theoretical shape for the focal spot of the corresponding annular aperture [34] with a radial obscuration ratio of 0.4 due to the use of a central stop. Compared to an unobscured circular aperture, this results in a slightly sharper focal spot but

#224406 - $15.00 USD Received 6 Oct 2014; revised 28 Nov 2014; accepted 1 Dec 2014; published 13 Jan 2015

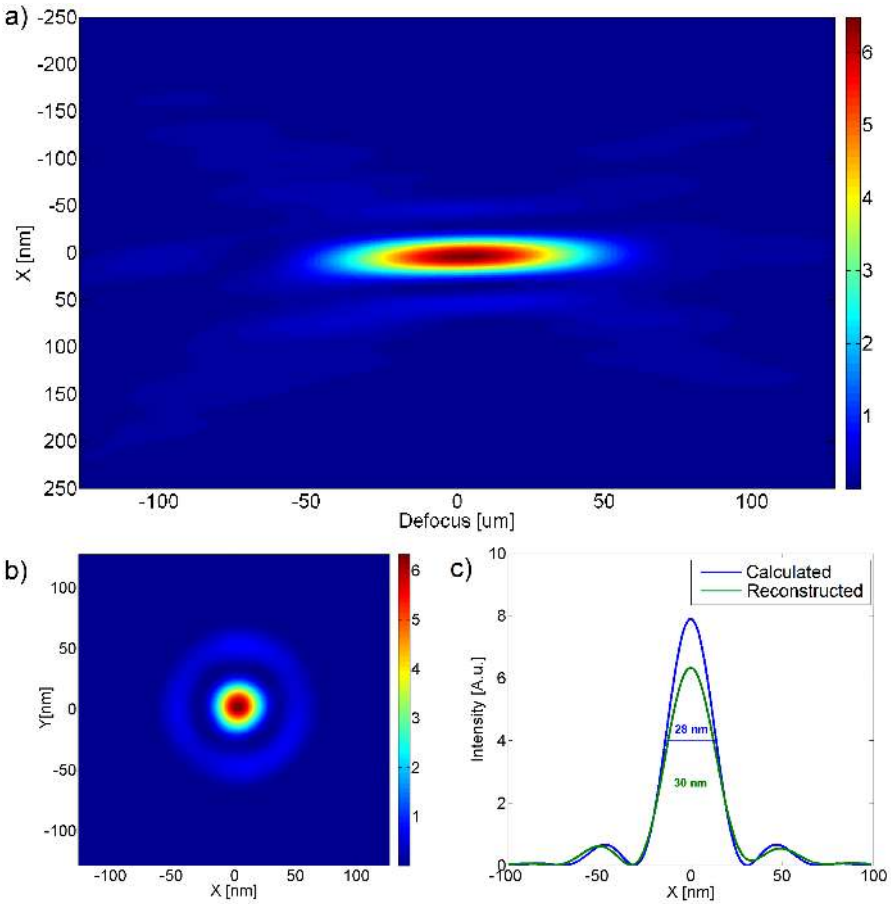

Fig. 6. Reconstructed and back-propagated probe wavefield of the best zone plate. (a) The intensity of the wavefield around the zone plate focus does not show obvious signs of aberrations. (b) and (c) The measured intensity profile of the focal spot is close to the theoretical profile of a lens with central obscuration. The measured 30 nm peak FWHM in in good agreement with the predicted value of 28 nm. The strong sidelobes are a consequence of using a central obscuration.

#224406 - $15.00 USD Received 6 Oct 2014; revised 28 Nov 2014; accepted 1 Dec 2014; published 13 Jan 2015

stronger sidelobes. As an optical benchmark, we used the Strehl ratio [35, 36], defined as the ratio of the measured peak intensity of the focal spot compared to the theoretically predicted value. The reconstructed ratio of 0.81 is considered to be within the diffraction limited range. This proves that our optics indeed match their nominal resolution and are free of aberrations.

3. Conclusions and outlook

We presented an approach to substantially increase the focusing efficiency of Fresnel zone plates in the hard X-ray range. The double-sided patterning of zone plates offers the advantages of stacked zone plates, while preserving a convenient and stable monolithic design. Presented high resolution double-sided zone plates have up to 9.9% focusing efficiency at 9 keV. This is twice the efficiency of their previously demonstrated single-sided counterparts. We have also proven that our lenses provide diffraction limited optical performance, and are capable to provide their nominal resolution. The improved photon efficiency provided by double-sided zone plates could help to push the resolution limit for radiation sensitive biological specimens in full-field microscopy, increase the measurement speed in scanning probe microscopy or provide a high numerical aperture illumination for coherent diffractive imaging [38]. Furthermore, the resolution of double-sided zone plates has a significant room for improvement, as both 10 nm zone width [23] and 2 nm overlay accuracy [17] have been demonstrated in the literature, paving the way towards efficient hard X-ray microscopy in the 10 nm range.

Acknowledgments

The authors are grateful to E. Deckardt and J. Lehmann for their assistance during sample preparation and to A. Diaz for her help during the presented measurements. Part of these experiments were performed at the cSAXS beamline at the Swiss Light Source, Paul Scherrer Institut, Villigen, Switzerland. We acknowledge SOLEIL for providing their synchrotron radiation facilities (Proposal ID: 99140070) and we would like to thank the staff of the Nanoscopium beamline for their support during these experiments. This research has received funding from the European Community's Seventh Framework Programme (FP7/2007-2013) under grant agreement No. 290605. (PSI-FELLOW/COFUND). This work was also supported by the Academy of Finland (Finnish Centre of Excellence in Atomic Layer Deposition and project 250968).

#224406 - $15.00 USD Received 6 Oct 2014; revised 28 Nov 2014; accepted 1 Dec 2014; published 13 Jan 2015